CMTC-486486-MS

Comparing Two Anionic Surfactants for Mobility Control With Supercritical CO_2 in Miscible EOR

Mohammed A. Almobarky, Zuhair Al Yousef, David Schechter, Texas A&M University

Abstract

Carbon Dioxide (CO_2) flooding is one of the most globally used EOR processes to enhance the oil recovery. However, the low gas viscosity and density result in gas channeling and gravity override which lead to poor sweep efficiency. Foam application for mobility control is a promising technology to increase the gas viscosity which leads to lower mobility and better sweep efficiency inside the reservoir. Foam is generated inside the reservoir by co-injection surfactant and gas. Although there are many surfactants that can be used for such purpose, their performance with Supercritical CO_2 ($ScCO_2$) is weak which leads to poor or loss of mobility control. This experimental study evaluates a newly developed surfactant (CNF) that was introduced for $ScCO_2$mobility control in comparison with a common foaming agent, anionic Alpha Olefin Sulfonate (AOS) surfactant. Experimental work was divided into three stages: foam static tests, interfacial tension measurements, and foam dynamic tests. Both surfactants were investigated at different conditions. In general, results showed that both surfactants are good foaming agents to reduce the mobility of $ScCO_2$ with better performance of CNF surfactant. Shaking tests in presence of crude oil showed that foam life for CNF extends to more than 24-hr but less than that for AOS. Moreover, CNF features lower CMC, higher adsorption and smaller area/molecule at the liquid-air interface. Furthermore, entering, spreading, and bridging coefficients interpretations indicated that CNF surfactant produces very stable foam with light crude oil in both DI and saline water, whereas AOS was stable only in DI water. At all conditions for mobility reduction evaluation, CNF exhibited stronger flow resistance, higher foam viscosity, and higher mobility reduction factor than that of AOS surfactant. In addition, CNF and $ScCO_2$ simultaneous injection produced 8.83% higher oil recovery than that of the baseline experiment and 7.87% higher than that of AOS. Pressure drop profiles for foam flooding using CNF was slightly higher than that of AOS indicating that CNF is better in terms of foam-oil tolerance which resulted in higher oil recovery.

Introduction

Oil reservoir has three recovery stages: primary, secondary and tertiary. After the primary and secondary stages, it is estimated that two-thirds of the OOIP are left underground (Green and Willhite 1998). For tertiary recovery, many Enhanced Oil Recovery (EOR) processes can be employed to extract more oil. Among these EOR processes, CO_2 injection is one the most utilized processes globally (Taber et al. 1997). However, gas injection processes face many challenges such as gas channeling and gravity override that lead to poor sweep efficiency (Healy et al. 1994). Many techniques have been applied to enhance the sweep efficiency such as water alternating gas (WAG), polymer, and foam. Foam is a promising technology that can be used to reduce the mobility of the injected gas by increasing its viscosity (Enick et al. 2012) and diverting the flow toward lower permeability zones where the remaining oil exists (Fried 1961).

The surfactant is the main element in foam system. It facilitates the foam generation by reducing the $\sigma_{g/w}$ which reduces the work required to generate foam, and it adsorbs at the interfaces to provide the foam with the required stability by stabilizing the thin-films between bubbles (Schramm, 2000).Thus, the surfactant screening is the first step toward successful surfactant-stabilized-foam project (Boeije et al. 2017). In foam applications, in general, and particularly in CO_2 EOR, surfactant structure is a significant factor that affects the efficiency in every aspect of the process: gas viscosity, mobility control, and EOR (Adkins et al. 2010). These effects are related to the different interactions of surfactants and CO_2 than that with air (Adkins et al. 2010). Moreover, $ScCO_2$ presence results in low pH acidic environment where some types of surfactants hydrolyze and lose their interfacial activity such as sulfates (Talley 1988).

Alpha olefin sulfonate (AOS) is hydrolytically and thermally stable, and soluble at low to medium hard water (Porter 1994). Farajzadeh et al. (2010) experimentally investigated the use of AOS for mobility control and EOR in miscible and immiscible flooding with the aid of CT scanner for simultaneous monitoring of the flooding process. They reported 19% more oil recovery with $ScCO_2$ than that of the immiscible CO_2 flooding. However, no sharp front was observed with the use of $ScCO_2$. They attributed this to the poor foam stability with oil. Haugen et al. (2012) experimentally used AOS for mobility control and EOR in fractured oil wet and water wet cores, and reported that the pre-generated foam is better than in-situ foam generation in terms of mobility reduction and oil recovery. They attributed the results to the poor foam-oil tolerance. Li et al. (2012) used AOS surfactant in Surfactant-Alternating-Gas (SAG) injection mode for foam generation using N_2. Their experiments were conducted in a two-dimensional sand pack with 19 to 1 permeability contrast. They attributed the poor sweep efficiency to the weak foam stability in presence of crude oil. They suggested that enhancing the foam-oil tolerance could provide higher oil recovery because this may enhance the sweep efficiency. Indeed, mixing the surfactant with a foam booster CTAB zwitterionic surfactant improved the foam-oil tolerance, provided better displacement efficiency, and resulted in higher oil recovery.

This study is to evaluate a newly developed anionic surfactant (CNF) to control the mobility of $ScCO_2$. Moreover, CNF surfactant results are compared with C14-16 AOS anionic surfactant which is heavily used in literature with CO_2 in gaseous and supercritical states. This new surfactant, and the major challenges for the surfactants' utilization with $ScCO_2$, may provide more opportunities for foam applications in foam-assisting miscible CO_2 EOR projects.

Materials

Table 1 shows the general properties of both surfactants used in experimental work. Surfactants were diluted using LabChem DI water ASTM, type II. Moreover, tests were conducted at 0.5-wt% surfactant concentration. Besides DI water, the salinity effect was investigated using brine solutions at 10,000, 20,000, and 30,000 ppm with Sodium Chloride (NaCl) purchased from Cole-Parmer. The crude oil used in this study is brought from North Burbank Unit, OK USA (NBU). It is light crude oil with 33.7°API, 8-cp viscosity at room temperature 23°C, and 39.5°API and 3.27-cp at 50°C which is the reservoir temperature. The properties of the glass-beads used to make the glass-beads pack are 2.5 specific gravity and 100-μm diameter purchased from Potters Industries LLC.

Table 1: The properties of the surfactants

Surfactant	Form	Chemical Family	pH	Density [gm/ml]	Charge	Flash Point [°C]	Carbon Chain Length
CNF	Liquid	Complex Nanofluid	7.73	1.07	Anionic	>93.3	--
AOS	Liquid	Alpha Olefin Sulfonate	8.2	1.06	Anionic	>94	14 -16

Methodology

The experimental work was divided into three stages: static foam tests, interfacial tension measurements, and foam dynamic tests. The foam dynamic tests are divided into three sections: mobility reduction evaluation in high permeability glass beads pack, mobility reduction evaluation in lower permeability Bentheimer sandstone, and core flooding experiments. As mentioned earlier, the surfactants concentrations were kept constant at 0.5-wt% diluted with DI water and prepared in three NaCl salinities: 10,000, 20,000 and 30,000 ppm.

Foam Static Tests

Foam was generated by shaking 3-ml of surfactant solutions in 13 X 100-mm (9-ml) Pyrex glass test tubes. Care has been taken to perform 10 to 15 gentle and uniform shakings for all samples. Samples were prepared at 0.5-wt% concentrations in DI water, 10,000, 20,000, and 30,000 NaCl brine solutions. After the foam has been generated with shaking inside the test tube, the foam columns were monitored by taking images at different times. Then, the foam columns lengths were measured from images using ImageJ software. The foaming ability was investigated using the initial foam column length (h_{fi}), and the foam stability was measured by the Foam Half-Life (FHL) which is the time at which the foam column loses half of the hfi. The samples were prepared for static tests without oil and stirred for about 12 hr before testing. For static tests with crude oil, the samples were prepared at 0.5-wt% concertation and stirred for 12-hr. Then, the surfactant solution is placed in 9-ml test tubes above which the crude oil was simply poured, then the sample was shaken immediately.

Interfacial Tension Measurements

Air-water surface tension measurements ($\sigma_{g/a}$) were conducted at different surfactant concentrations in DI water using Dataphysics OCA 15 Pro IFT instrument, pendant drop method. The surface measurements

were used for CMC determination and interfacial activity predictions for both surfactants.

The surface tension $\sigma_{a/w}$ measurements vs. the logarithmic values of the concentrations below the CMC is a linear relationship with a straight line. The slope of this straight line can be used to interpret the interfacial activities: adsorption and area/molecule at the interface. According to Gibbs adsorption equation, the higher the slope is the higher the adsorption at the air-water interface. Furthermore, the higher the adsorption at the density also results in smaller area/molecule which indicates a stronger packing at the interface which induces higher foam stability (Rosen and Kunjappu 2004).

The interfacial tension measurements, also, can be also used to investigate the foam-oil tolerance by calculating the entering coefficient (E), spreading coefficient (S), bridging-coefficient (B), and the lamellae number (L) using equations 1, 2, 3, and 4 below where $\sigma_{o/w}$ and $\sigma_{o/g}$ are the oil-water and oil-gas interfacial tension, respectively.

$$E=\sigma_{a/w}+\sigma_{o/w}-\sigma_{o/g} \quad (1)$$

$$S=\sigma_{a/w}-(\sigma_{o/w}+\sigma_{o/g}) \quad (2)$$

$$B=\sigma^2_{a/w}+\sigma^2_{o/w}-\sigma^2_{o/g} \quad (3)$$

$$L=0.15\,\frac{\sigma_{a/w}}{\sigma_{o/w}} \quad (4)$$

Foam Dynamic Tests

These experiments were designed for mobility reduction evaluation and oil recovery investigation by conducting core flood experiments.

Mobility Reduction Evaluation in High Permeability Glass Beads Pack

These experiments were conducted at different shear rates 317-sec^{-1}, and one low shear rate 9.51-sec^{-1}. Furthermore, three injection qualities were applied 50, 70, and 90%. All experiments were conducted at constant pressure and temperature 1800-psi and 50°C to ensure the supercritical conditions of CO_2. The foam was generated by simultaneously injecting surfactant and $ScCO_2$ through the glass beads pack. The pressure drop was measured using two sets of pressure transducers: 500-psi for high range and 50-psi for low range. The pressure drop data were collected using data acquisition system. The onset of strong foam generation was recognized as a rapid increase in pressure drop according to Dicksen et al. (2002). The flow continued with monitoring the pressure drop data until the steady state pressure was attained. Then, the steady state pressure drop collected data were averaged and used to calculate the mobility, foam effective viscosity, and Mobility Reduction Factor (MRF) using equations 5, 6 and 7 below.

$$\lambda=\frac{k}{\mu}=\frac{q\,l}{A\,\Delta P} \quad (5)$$

$$\mu_{eff}=\frac{k}{\lambda} \quad (6)$$

$$MRF=\frac{\Delta P_{foam}}{\Delta P_{baseline}} \quad (7)$$

Where λ for mobility, k is the permeability, μ viscosity, q is the flow rate, *l* is the length of the porous media, A is the cross sectional area of the glass beads pack

Table 2 shows the dimensions and the petrophysical properties.

Table 2: Glass beads properties

Glass Beads Size	100 μm
Length	13 in
Diameter	0.18 in
Pore Volume	1.625 ml
Porosity	30%
Permeability	17.1 -Darcy

Figure 1 below show the experimental setup for the mobility reduction evaluation.

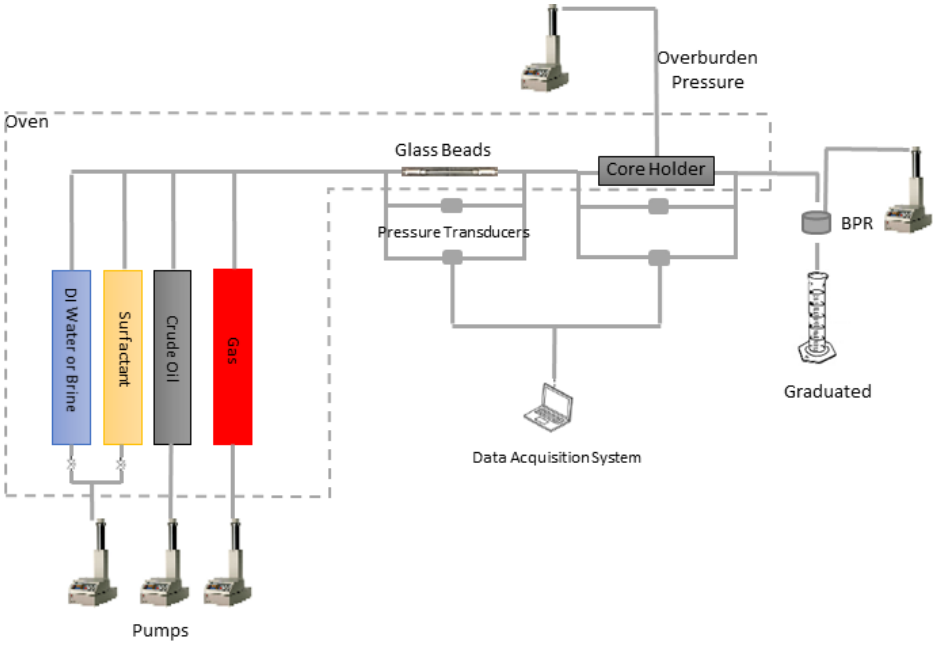

Figure 1: Mobility reduction evaluation and core flooding experimental setup

Table 3 shows the experimental conditions for the experiments conducted in the glass beads pack for mobility reduction evaluation at 317-sec^{-1} and 9.51-sec^{-1} shear rates. Run No. 20 is the base line experiment at which ScCO2 were used without surfactant for comparison purposes.

Table 3: Glass beads pack experimental conditions

Run #	Surfac-tant	Salinity NaCl [wt%]	Injection Quality [%]	Q [ml/min]	Shear rate [1/sec]
1	AOS	--	90	0.5	317
2	AOS	1	90	0.5	317
3	AOS	2	90	0.5	317
4	AOS	3	90	0.5	317
5	AOS	--	70	0.5	317
6	AOS	1	70	0.5	317
7	AOS	2	70	0.5	317
8	AOS	3	70	0.5	317
9	AOS	--	50	0.5	317
10	AOS	1	90	0.015	9.51
11	CNF	--	90	0.5	317
12	CNF	3	90	0.5	317
13	CNF	1	90	0.015	9.51
14	--	1	--	0.5	317

Mobility Reduction Evaluation in Low Permeability Bentheimer Sandstone

These experiments were conducted using 1" diameter 12" length homogeneous Bentheimer sandstone. The core was left in an oven overnight for drying. Then, it was mounted in the core holder and 500-psi overburden pressure was applied. After that, the air was removed from the core using vacuum pump followed by saturating the core with 10,000 ppm NaCl brine solution at which the pore volume and porosity can be measured. Then, the overburden pressure was kept at 500-psi more than the test pressure, the experimental setup along with the core was pressurized using the back pressure regulator, as shown in figure 1. Experimental conditions for all runs are listed in Table 4. After the system was pressurized and the temperature was maintained at 50°C, the absolute permeability was measured by obtaining the pressure drop at different flow rate using Darcy law. Then, 5 to 6 pore volumes of brine solution were injected to ensure 100% core saturation. Although the XRD tests for these rocks showed that their composition is 100% quartz, 1 pore volume of surfactant solution was injected into the core at 5 ft/day (~ 9-sec-1 shear rate) to mitigate the effect of surfactant adsorption on rock surfaces. After that, the foam was applied by simultaneously injecting surfactant and $ScCO_2$ or N_2 gas at 5 ft/day, too. The foam injection was continued until the steady pressure was attained. The recorded steady state pressure drop data were averaged and used to calculate the mobility, foam effective viscosity, and MRF using equations 5, 6, and 7 above. Figure 1 above shows a schematic diagram of the experimental setup for mobility evaluation in sandstone. Table 4 below shows the properties and the experimental conditions for the experiments conducted in Bentheimer sandstone. Moreover, the last two experiments in Table 4 (runs 9 and 10) are baseline experiments conducted using N_2 and $ScCO_2$ injection for comparison purposes, respectively. Table 4: Petrophysical properties for Bnetheimer Sandstone in mobility reduction evaluation and experimental conditions

Table 4: Petrophysical properties for Bnetheimer Sandstone in mobility reduction evaluation and experimental conditions

Run #	Surfac-tant	Concentr-tion [wt%]	NaCl Salinity [wt%]	P [psi]	Velocity [ft/day]	ShearRate [sec^{-1}]	Injection Quality [%]	Gas	K [Darcy]
1	AOS	0.5	1	1800	5	8.92	90	$ScCO_2$	1.7
2	AOS	0.5	1	1800	5	8.92	70	$ScCO_2$	1.58
3	CNF	0.5	1	1800	5	8.92	90	$ScCO_2$	1.7
4	CNF	0.5	1	1800	5	8.92	70	$ScCO_2$	1.7
5	AOS	0.5	1	850	5	9	90	N_2	1.57
6	AOS	0.5	1	850	10	18	90	N_2	1.57
7	CNF	0.5	1	850	5	9.	90	N_2	1.7
8	CNF	0.5	1	850	10	18	90	N_2	1.7
9	--	--	1	850	5	9	--	N_2	1.62
10	--	--	1	1800	5	9	--	$ScCO_2$	1.62

Core Flooding Experiments

The core flooding experiments were also conducted in 1" diameter 12" length homogeneous Bentheimer sandstone. The core was left in an oven overnight for drying. Then, it was saturated with water following the same procedure conducted in the mobility reduction evaluation. After that, 5 to 6 pore volumes were injected into the core at a low flow rate to ensure 100% water saturated porous media followed by the absolute permeability measurement using Darcy law. The setup was pressurized to 1450-psi keeping the overburden pressure 500-psi higher than the test pressure, and the test temperature was 50°C. Once the

pressure and temperature were stable, crude oil was injected at 5 ft/day until no more water was observed in the effluent. The water production was collected in a graduated cylinder for the OOIP estimation. Then, water flooding was applied by injecting 5 pore volumes of brine solution at 5 ft/day until no more oil production was observed. The high amount of water injection was to ensure that water flooding reached the optimum oil recovery, no more oil can be produced by water injection, and to ensure the removal of any end effects might exist. Then, the second stage was to inject 1 to 1.5 pore volumes of the surfactant solution (surfactant pre-flush) to mitigate the surfactant adsorption on the rock. After that, 5 pore volumes of simultaneous injection of surfactant and $ScCO_2$ was applied for 24-hr at 5 ft/day. Pressure drop was recorded for the three oil recovery stages. Figure 1 shows the schematic diagram for the core flooding experimental setup. One baseline experiment was conducted by injecting $ScCO_2$ only for comparison purposes with oil recovery of CNF and AOS foam floods. Table 5 shows the properties for the Bentheimer sandstone used to conduct the core flooding experiments and the experimental conditions.

Table 5: Petrophysical properties for the Sandstone and the experimental conditions in core flooding experiments.

Run #	Surfactant	Length [in]	Diameter [in]	Pore Volume [cc]	Porosity [%]	Permeability [Darcy]	Type
1	--	12	1	33.52	21.71	1.87	Baseline
2	AOS	12	1	34.74	22.5	1.71	Foam Flood
3	CNF	12	1	33.74	21.85	1.91	Foam Flood

Results and Discussion

Foam Static Tests

Foaming Ability (or foamability) was investigated by measuring the initial foam heights (h_{fi}) for both surfactants from the shaking tests. Both surfactants gave almost the same h_{fi}. Therefore, both CNF and AOS are good foaming agents in terms of foaming ability. This also indicates the efficiency of both surfactants to reduce the air-liquid surface tension. The surface tension at the air-liquid interface will be discussed shortly.

Figure 2 shows the FHL for both surfactants in DI water, 10,000, 20,000, and 30,000 ppm NaCl salinities. Both surfactants provided good foam stability. As observed, foam stability decreases as the salinity increase which is attributed to the reduction in repulsive forces between the surfactant molecules due to the addition of salts. Moreover, CNF surfactant is slightly better than AOS in DI water and in all salinities. For both surfactants, DI water foam stability is the best. Foam stability decreases with the addition of salts and with increasing the salinity up to 20,000 ppm, but both surfactants exhibited foam stability enhancement at 30,000 ppm NaCl. Liu et al. (2005) reported that foam stability with CO_2 decreased with increasing salinity up to 2-wt%. Then, a further increase in salinity enhanced the foam stability. However, foam stability plateaued shortly with further increase in salinity. Zhao et al. (2012) reported that the developed surfactant mixture exhibited better stability as the salinity increased, whereas a further increase in salinity weakens the foam stability considerably.

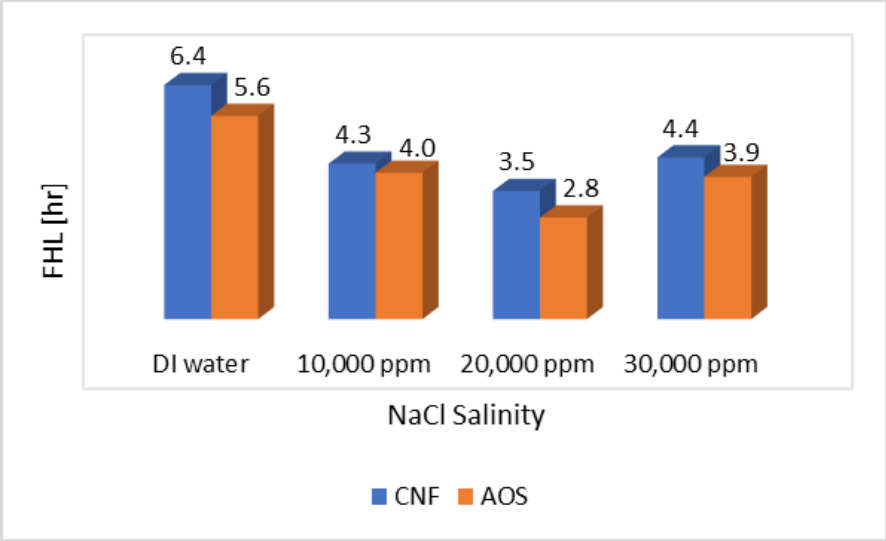

Figure 2: Foam half-lives or both surfactants in DI water, 10,000, 20,000, and 30,000 ppm at 0.5-wt% concentrations.

The foam stability with crude oil was impressive for both surfactants with FHL extends to more than a day for CNF and 12 -18 hr for AOS. Figure 2 shows two images for CNF left and AOS right. CNF image was taken after 24-hr, whereas AOS image were taken after 18-hr. Each image shows samples in DI water, 10,000, and 20,000 ppm salinity left to right. Clearly, both surfactants produced stable foam with crude oil, but CNF foam was significantly stronger than that of AOS in presence of crude oil.

However, shaking involves eventually very high shear rates which provide high energy for any surfactant to give its optimum performance as foaming agents regardless of how the shaking was performed. Therefore, it is difficult to recognize the differences in foaming ability and foam stability as well. Therefore, combining the shaking tests observations with the interfacial tension measurements are next.

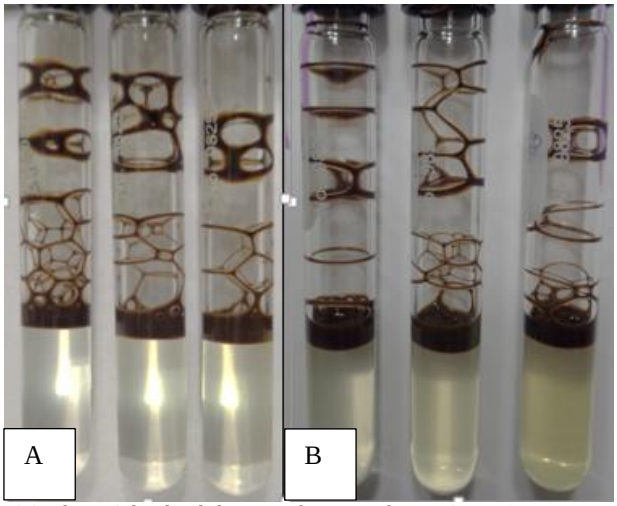

Figure 3: A) CNF after 24-hr and B) AOS after 18-hr, both images for samples at 0.5-wt% concentration in DI water, 10,000 and 20,000 ppm.

Interfacial Tension Measurements.

As mentioned earlier, surface tensions were measured a different concentrations for samples prepared in DI water. The measurements are shown in surface tension vs. log (concentration) plot in Figure 4. The

CMC values for CNF and AOS are 0.011-wt% and 0.028-wt%, respectively. Surfactant concentration for foam application are recommended above the CMC (Nikolov et al. 1986). Using surfactant concentration above the CMC provides the best foam stability, whereas foam has less opportunity to be of good stability when using surfactant concertation below the CMC (Rafati et al. 2012). The CMC defines the foaming efficiency of the surfactants. The lower the CMC is the higher the foaming efficiency (Rosen and Kunjapoo 2004). Moreover, Mannhardt et al. (2000) found experimentally the foaming ability decreases with decreasing the concentrations and no foam generation would be possible for concentrations below the CMC. Therefore, the lower the CMC of the surfactant the better in many ways but the most important is lowering the project costs as the lower CMC enables the use lower surfactant concentrations for good foaming efficiency.

According to Gibbs surface adsorption equation 8, the higher the slope is the higher the adsorption of the surfactant at the liquid-air interface, and consequently, the better the foamability and foam stability (Rosen and Kunjappo 2004). Moreover, the higher the adsorption of a foaming agent at the air-liquid interface is the smaller the area/molecule at the interface. Therefore, such properties in a foaming agent indicate that it provides better foam stability because of the smaller area/molecule which has stronger packing of the foaming agent molecules at the interface.

$$\Gamma = -\frac{1}{RT}\left(\frac{d\gamma}{d\ln C}\right) \qquad (8)$$

Where Γ surfactant adsorption at the air-liquid interface, R: gas constant, T temperature, ϒ: surface tension and C concentration.

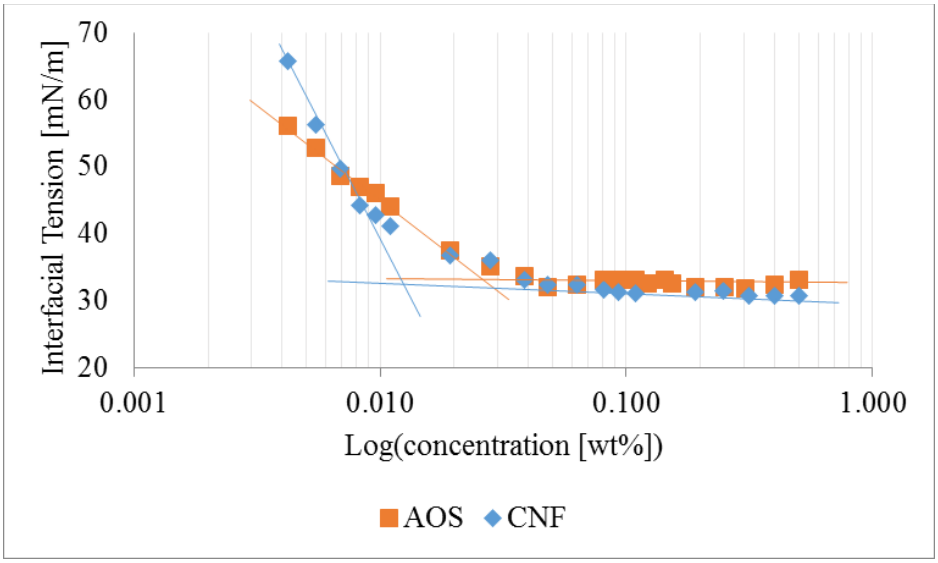

Figure 4: Interfacial measurements for AOS and CNF

Furthermore, for almost all concentrations in **figure 4**, CNF is able to reduce the surface tension lower than that of AOS which also indicates that CNF is predicted to perform better than AOS in foam generation. Table 6 and 7 show the $\sigma_{a/w}$ for both surfactants at 0.5-wt% concentration in DI and saline water.

Table 6: O/W and A/W IFT for AOS surfactant concentration at 23°C

		NaCl Salinity [ppm]		
	DI Water	10,000	20,000	30,000
$\sigma_{a/w}$	32.5	32.3	32.1	32.15
$\sigma_{o/w}$	1.4	0.52	0.44	0.38

***Table 7*: $\sigma_{a/w}$ and $\sigma_{o/w}$ for CNF at 0.5-wt% surfactant concentration at 23°C**

		NaCl Salinity [ppm]		
	DI Water	**10,000**	**20,000**	**30,000**
$\sigma_{a/w}$	30.7	31	31.25	31.11
$\sigma_{o/w}$	5.88	3.94	3.51	3.11

Foam Stability in Presence of Crude Oil.

Table 6 and 7 show the $\sigma_{o/w}$ measurements for both surfactants in DI and saline water. The addition of salts with CNF showed no much reduction in $\sigma_{o/w}$ as in AOS. This means that CNF has high probability to be more efficient in terms of foam-oil tolerance inside the reservoir.

Tables 8, 9, 10, and 11 show the entering, spreading, bridging coefficients and lamellae number, respectively. Table 8 for entering coefficient gives positive values for all which clarifies that oil will enter the lamellae. However, table 9 for spreading coefficient implies that oil will spread at the A/W interface to destabilize the foam for AOS foam in saline solutions only. The spreading coefficient for CNF is negative for all samples. Moreover, table 10 gives negative values for CNF at all conditions. These observations imply that CNF is going produce very stable foam with oil. However, AOS produces stable foam with oil in DI water. Furthermore, lamellae number values in table 11 confirm the same. CNF foam are in stable region in DI water, and all samples in salinities are in the semi-stable regions. However, AOS in DI water is in the semi-region, and unstable for all samples in saline water.

***Table 8*: Entering coefficients at 0.5-wt% surfactant concentration at 23°C**

		NaCl Salinity [ppm]		
Surfactant	**DI water**	**10,000**	**20,000**	**30,000**
AOS	2.4	1.32	1.04	1.03
CNF	5.08	3.44	3.26	2.72

***Table 9*: Spreading coefficients at 0.5-wt% surfactant concentration at 23°C**

		NaCl Salinity [ppm]		
Surfactant	**DI water**	**10,000**	**20,000**	**30,000**
AOS	-0.4	0.28	0.16	0.27
CNF	-6.68	-4.44	-3.76	-3.5

***Table 10*: Bridging coefficients at 0.5-wt% surfactant concentration at 23°C**

		NaCl Salinity [ppm]		
Surfactant	**DI water**	**10,000**	**20,000**	**30,000**
AOS	65.96	51.31	38.35	41.52
CNF	-15.19	-15.73	-3.37	-14.75

***Table 11*: Lamellae number at 0.5-wt% surfactant concentration at 23°C**

	NaCl Salinity [ppm]			
Surfactant	**DI water**	**10,000**	**20,000**	**30,000**
AOS	3.48	9.32	10.94	12.69
CNF	0.78	1.18	1.34	1.50

Foam dynamic Tests in Glass Beads Pack (High Permeability)

Fourteen runs were conducted in the high permeability glass beads pack at high and low shear rates for both surfactants with $ScCO_2$ foam. Moreover, one baseline experiment at which the $ScCO_2$ injection was not able to provide measurable pressure data unless at 317-sec^{-1} high shear rate. The comparisons below are made based on the foam effective viscosities measured using the steady state pressure drop across the glass beads pack. Results are listed in table 12 below and the experimental conditions for these tests are listed previously in table 3.

Table 12: Experimental Conditions and results for AOS and CNF with CO_2 in Glass beads pack

Run #	Surfac-tant	Salinity NaCl [wt%]	Injection Quality [%]	Q [ml/min]	Shear rate [1/sec]	ΔP_{ss} [psi]	Mobility [md/cp]	μ_{eff} [cp]	MRF
1	AOS	--	90	0.5	317	208	118	144	5225
2	AOS	1	90	0.5	317	164	150	114	4100
3	AOS	2	90	0.5	317	161	156	109	4025
4	AOS	3	90	0.5	317	216	459	37	5400
5	AOS	--	70	0.5	317	175	142	121	4375
6	AOS	1	70	0.5	317	99	249	69	2475
7	AOS	2	70	0.5	317	93	265	64	2325
8	AOS	3	70	0.5	317	91	273	63	2275
9	AOS	--	50	0.5	317	122	202	85	3050
10	AOS	1	90	0.015	9.51	9.97	74.15	230	250
11	CNF	--	90	0.5	317	162	153	112	4050
12	CNF	3	90	0.5	317	118	209	82	2950
13	CNF	1	90	0.015	9.51	16.09	46.00	371	402
14	--	1	--	0.5	317	0.04	616,270	0.03	--

The effect of injection quality is shown Figure 5. It shows the effect of three injection qualities on both surfactants' foam viscosities at high shear rate in DI water. AOS foam viscosity decreases as the injection quality decreases, whereas CNF foam viscosity increases as the injection quality increases. The opposite behaviors of these foaming agents can be attributed to many reasons that were not covered in this study. In fact, the relationship of the foam viscosity with injection quality is still controversial. In an experimental work conducted by Marsden and Khan (1966), they found that the higher the injection quality is the higher the foam viscosity. Lee and Heller (1990) experimentally found the opposite where the increase in injection quality decreases the viscosity. Foam viscosity depends on factors such flow rate, the permeability of the porous media, and foam texture (Hirasaki and Lawson 1985).

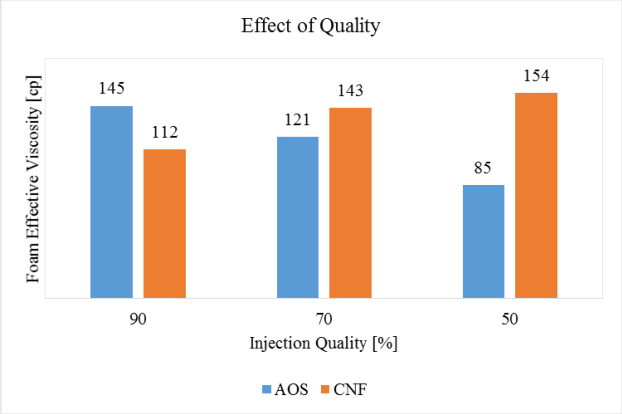

Figure 5 : Effect of injection quality of AOS and CNF in glass beads pack at 317-sec^{-1}

The effect of shear rate at 90 % injection quality for both AOS and CNF at high shear rate 317-sec^{-1} and low shear rate 9.51-sec^{-1} at 10,000 ppm NaCl salinity are shown in Figure 6. The higher the shear rate is the lower viscosity because of the shear thinning nature of foam. As shown, foam viscosities of CNF at both shear rates are better than that of AOS. Figure 7 also shows all results for CNF and AOS at low shear rate 9.51-sec^{-1} at 90% injection quality in 10,000 ppm NaCl salinity. Again, CNF proves its powerful performance with higher steady state pressure drop, lower mobility, higher foam viscosity, and higher mobility reduction factor (MRF).

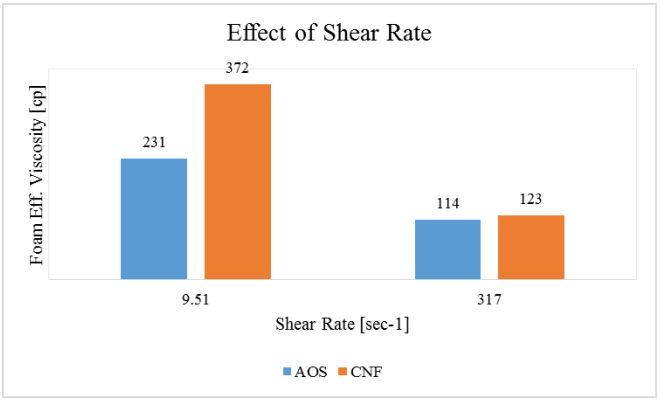

Figure 6 : High vs. low shear rate foam viscosities for AOS and CNF at 0.5-wt% surfactant concentration at 90% injection quality

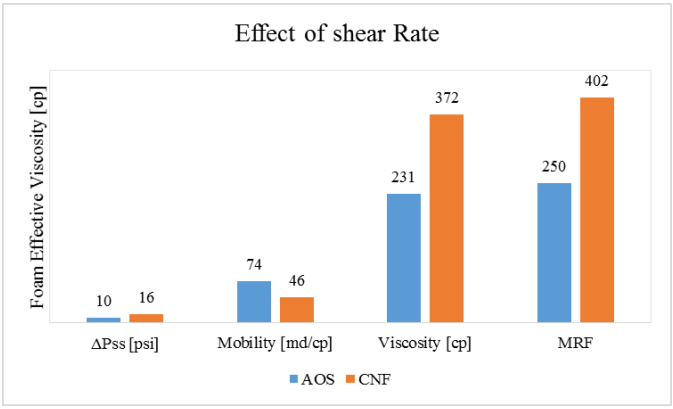

Figure 7: low shear rate results at 0.5-wt% surfactant concentration at 90% injection quality

Foam Dynamic Tests in Bentheimer Sandstone (low Permeability)

Two among 10 experiments were conducted using N_2 injection at 850-psi and $ScCO_2$ injection at 1800-psi as baseline experiments for comparison. All experimental conditions are listed in table 4. Results are listed in table 13.

***Table 13*: Experimental Conditions for AOS and CNF in sandstone**

Run #	Surfactant	Gas	Injection Quality [%]	ΔP_{ss} [psi]	Mobility [md/cp]	Foam Viscosity [cp]	MRF
1	AOS	$ScCO_2$	90	0.4	411	4.13	1.67
2	AOS	$ScCO_2$	70	25.42	6.79	237.11	105.9
3	CNF	$ScCO_2$	90	0.60	301.06	7.21	2.5
4	CNF	$ScCO_2$	70	2.00	89.00	20.00	8.3
5	AOS	N_2	90	1.35	129.98	12.69	3.4
6	AOS	N_2	90	3.46	101.43	16.27	8.6
7	CNF	N_2	90	12.89	13.61	124.88	32.2
8	CNF	N_2	90	34.4	10.20	166.64	86
9	--	N_2	--	0.4			--
10	--	$ScCO_2$	--	0.24	680	2.5	--

The effect of permeability is shown in Figure 8 which compares the foam viscosities for AOS and CNF with $ScCO_2$ at 90% injection quality at 9-sec^{-1} shear rate. The permeabilities of the cores and glass beads pack are 1.7 to 1.98 Darcy and 17.1-Darcy, respectively. CNF is repeatedly prove to be better than AOS by generating higher foam viscosity in both cases at high and low permeability porous media. These results in figure 8 are in agreement with the fact that foam favors the higher permeability. The foam viscosities for surfactants in the glass beads pack are extremely higher than that in sandstone.

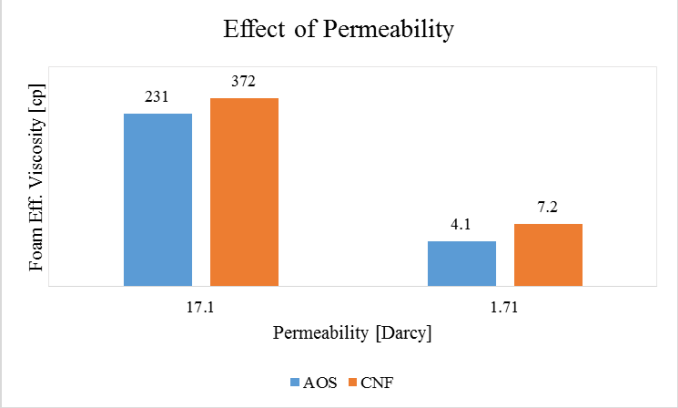

Figure 8: AOS and CNF at ScCO2 at 90% injection quality

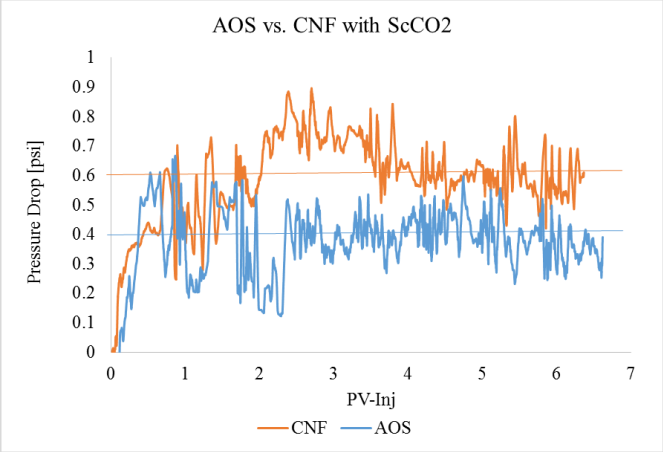

Figure 9: AOS and CNF at ScCO2 at 90% injection quality in sandstone

The effect of injection quality at low permeability sandstone were investigated using two injection qualities 90% and 70% for both surfactants with $ScCO_2$ at 9.51 sec^{-1} shear rate. The pressure profiles for both surfactants are shown in Figures 9 for 90% and 10 for 70% injection quality. According to the pressure profiles, CNF foam is stronger at 90%, whereas AOS is stronger at 70% injection quality. Therefore, the results suggest that CNF is better at more realistic conditions (i.e. low shear rate and sandstone reservoir), CNF co-injection with $ScCO_2$ provide higher foam viscosity at higher injection qualities, while AOS requires low injection qualities for better performance. This also indicates that using CNF for mobility control with $ScCO_2$ will eventually reduce the cost as the amount of liquid decreases as the injection quality increases.

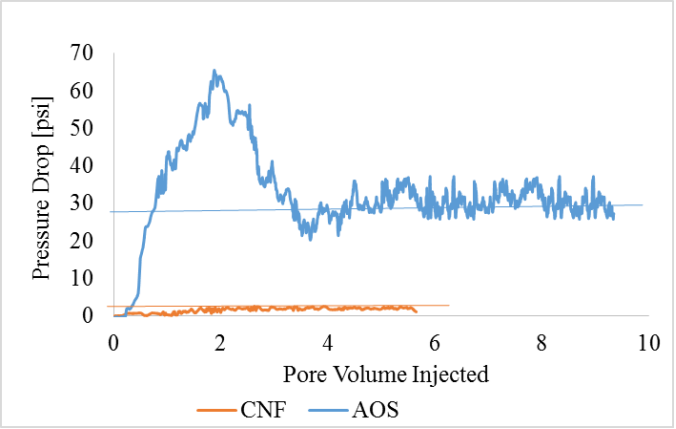

Figure 10: AOS and CNF at ScCO2 at 70% injection quality in sandstone

The mobility control with N_2 gas was also tested for both surfactants. The pressure profiles for AOS and CNF are shown in Figure 11. These experiments were conducted in sandstone at 0.5-wt% surfactant concentrations prepared in 10,000 ppm NaCl brine solution at two velocities 5 and 10 ft/day (9 and 18-sec^{-1}) at 90% injection quality. Each surfactant was injected simultaneously with N_2 gas at 5 ft/day until the steady state pressure drop was attained, then the velocity was raised to 10 ft/day until the steady state pressure drop was attained for the new velocity. From Figure 11, CNF appeared always better in terms of flow resistance at both velocities than AOS. Moreover, Figure 12 compares the foam viscosities for AOS and CNF at both velocities. Surprisingly, the viscosity increases as the velocity (i.e shear rate) increases for both surfactants. Although this is shear thickening behavior, foam is known of its non-Newtonian shear

thinning nature (Schramm and Wassmuth 1994). This behavior could be related to the procedure of the experimental work. Precisely, the reason could be performing two velocities in one experiment. At 5 ft/day, the surfactant was very efficient to provide high flow resistance due to the gas blockage effect. Therefore, the gas relative permeability is already low, and increasing the velocity to 10 ft/day at such conditions would promote the foam generation because of the high shear rate in a blocked porous media. As a result, foam contradicted its shear thinning nature by providing higher viscosity at higher shear rate, lesson learned.

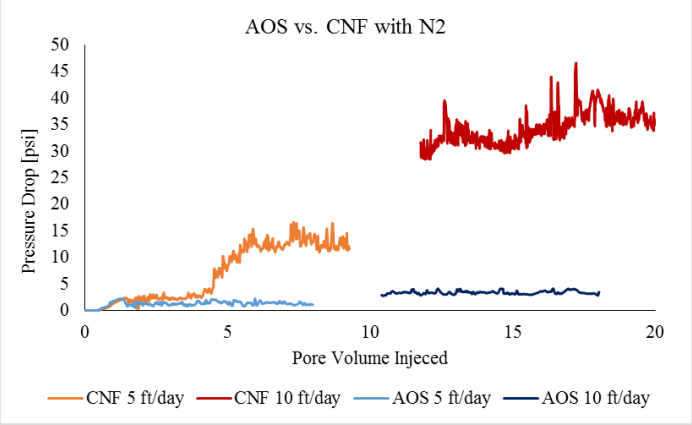

Figure 11: AOS and CNF with N2 at 850-psi at 5 and 10 ft/da velocities at 90% injection qualities

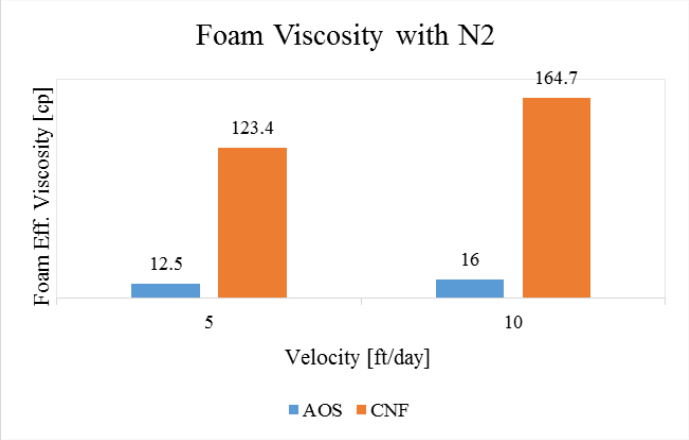

Figure *12*: Foam viscosity at 5 and 10 ft/day for 0.5-wt% of CNF and AOS in 1-wt% NaCl brine solution at 90% injection quality with N_2 gas

Core Flood Experiments

The baseline experiment oil recovery is shown as a function of pore volume injected in Figure 13. The ultimate oil recovery of water flooding is 36% of the OOIP. The water flooding was followed by 5 to 6 pore volume of continuous $ScCO_2$ injection which resulted in 27.54% of the OOIP more oil recovery. The total oil recovery from the baseline experiment is 76.2% of the OOIP.

Figure 14 shows the results for AOS as a foaming agent after water flooding. The same procedure were conducted. This run started with injecting 4.56 pore volumes of water, water flooding, which resulted is 35.42% of the OOIP oil recovery. Then, 1.62 pore volume of AOS surfactant solution were injected to reduce the surfactant adsorption on the rock surfaces. The surfactant pre-flush stage resulted in 4.75% of the OOIP oil recovery. The third stage is the foam flood with simultaneous injection of 5 pore volumes of

AOS/$ScCO_2$. AOS foam flood resulted in 28.5% additional oil recovery, and 68.67% of the OOIP total oil recovery. The additional recovery by AOS foam accounts for 1% higher than that of baseline experiment.

CNF foam core flood results are shown in figure 15. Water flooding stage produced 39.66% of the OOIP. Moreover, no oil production was observed during the injection of around 1.5 pore volumes of CNF solution to reduce the adsorption effect. The final stage, CNF-$ScCO_2$ simultaneous injection or foam flooding resulted in 36.3% of the OOIP oil recovery after water flooding. This amount of oil produced by CNF foam is 7.87% higher than that of AOS foam, and 8.83% higher than baseline experiment. The total recovery for this core flood is 76.3%.

In addition, the pressure drop for the recovery stages in foam core floods are shown in figure 14 and 15. The CNF foam pressure drop in figure 15 is slightly higher than that of AOS foam in figure 14. Both pressure drops are high enough o CNF foam in figure 16 and AOS foam in figure 15. However, during the last 1 pore volume, the CNF foam pressure drop maintained higher pressure drop than that of AOS foam. This is attributed to the higher CNF foam stability with oil.

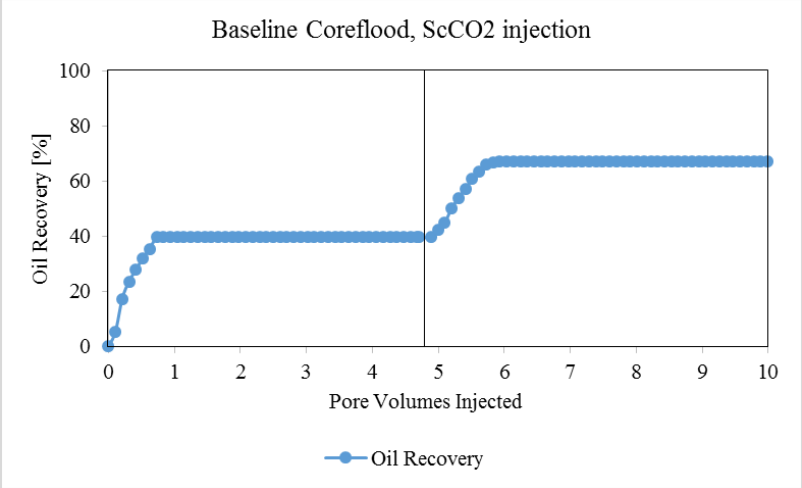

Figure 13: Baseline experiment

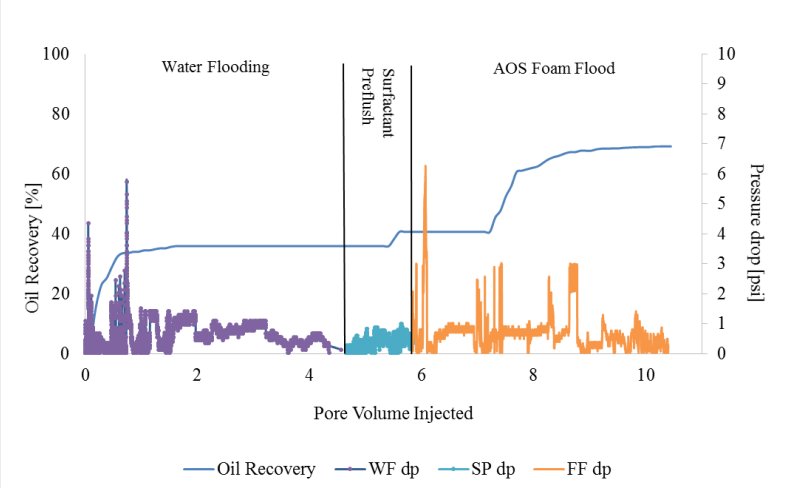

Figure *14*: AOS foam flood experiment

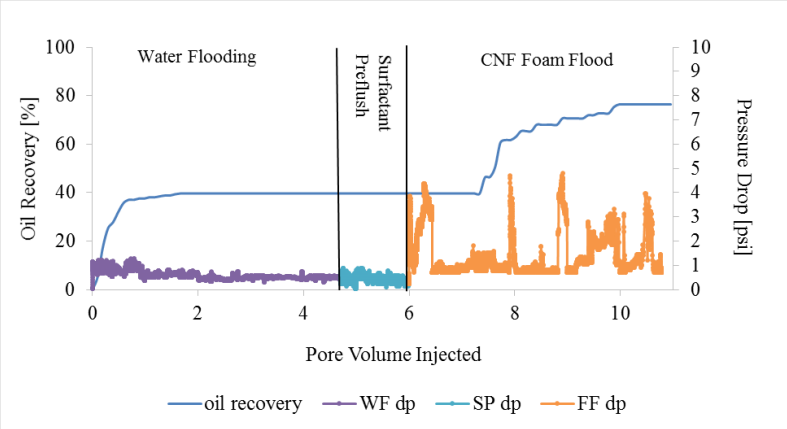

Figure 15: CNF foam flood experiment

Conclusion

1. This study investigated two surfactants for the mobility control with $ScCO_2$: CNF newly developed surfactant and the foaming agent anionic surfactant AOS.
2. Both surfactants showed good foaming ability and foam stability without oil in shaking tests. Such behavior is not representative to the actual foaming ability of both surfactants because the shaking tests are naturally involved high shear rate which enforce the surfactants to perform at their optimum abilities as foaming agents. However, CNF was able to reduce the A/W IFT lower than that of AOS.
3. The newly developed surfactant, CNF, showed impressive foam oil tolerance than AOS. It does not reduce the O/W IFT to low value same as AOS in saline water. This makes it a good surfactant for the applications of mobility control.
4. CNF provided negative values of entering, spreading, and bridging coefficients, whereas AOS provided negative values in DI water only. Moreover, lamellae number indicates that CNF foam is stable in DI water and semi-stable with the addition of salts in terms of foam-oil tolerance. However, the lamellae number for AOS showed semi-stable in DI water, and unstable at all salinities. These results showed that CNF is very stable with oil more than AOS.
5. At all conditions for mobility reduction with $ScCO_2$, and with N_2 at lower pressures, CNF showed higher foam viscosity, and better mobility reduction than AOS.
6. For oil recovery with $ScCO_2$ mobility control, AOS produced 1% more than the baseline experiment, whereas CNF produced almost 7.78% more than AOS foam, and 8.38% more than the baseline experiments.
7. It is not recommended to test two shear rates at one experiment. Such procedure would result in dramatic errors in foam viscosity measurements.

Nomenclature

OOIP	original oil in place
EOR	enhanced oil recovery
CNF	complex nanofluid

AOS	alpha olefin sulfonate
$ScCO_2$	supercritical CO_2
MRF	Mobility reduction factor
DI	deionized water
API	American petroleum institute
Ppm	part per million
Ml	milliliter
$\sigma_{g/w}$	gas-water interfacial tension
$\sigma_{o/w}$	oil-water interfacial tension
$\sigma_{o/g}$	oil-gas interfacial tension
h_{fi}	initial oam height in shaking tests
FHL	foam half life
E	entering coefficient
S	spreading coefficient
B	bridging coefficient
L	lamellae number

References

Adkins, S. S., Chen, X., Nguyen, Q. P., Sanders, A. W., & Johnston, K. P. 2010. Effect of branching on the interfacial properties of nonionic hydrocarbon surfactants at the air–water and carbon dioxide–water interfaces. Journal of Colloid and Interface Science, 346 (2), 455-463. DOI: 10.1016/j.jcis.2009.12.059

Bera, A., Ojha, K., & Mandal, A. 2013. Synergistic Effect of Mixed Surfactant Systems on Foam Behavior and Surface Tension. *Journal of Surfactants and Detergents.* **16** (4): 621-630.

Boeije, C. S., Bennetzen, M., & Rossen, W., 2017. A Methodology for Screening Surfactants for Foam Enhanced Oil Recovery in an Oil-Wet Reservoir. doi: 10.2118/185182-pa.

Dicksen, T., Hirasaki, G. J., & Miller, C. A. 2002. Conditions for Foam Generation in Homogeneous Porous Media. SPE/DOE Improved Oil Recovery Symposium, 13-17 April, Tulsa, Oklahoma, USA. SPE-75176-MA.

Enick, Robert Michael, David Kenneth Olsen, James Robert Ammer et al. 2012. Mobility and Conformance Control for CO_2 EOR via Thickeners, Foams, and Gels -- A Literature Review of 40 Years of Research and Pilot Tests. SPE Improved Oil Recovery Symposium, Tulsa, Oklahoma, USA. SPE-154122-MS.

Farajzadeh, R., A. Andrianov, and P. L. J. Zitha. 2010. Investigation of Immiscible and Miscible Foam for Enhancing Oil Recovery. Industrial & Engineering Chemistry **49** (4): 1910-1919.

Fried, A. N. The Foam-Drive Process for Increasing the Recovery of Oil. 1961. U.S. Bureau of Mixes, Rep. Inv., 5866, Washington, D. C.

Hirasaki, G., Lawson J. 1985. Mechanisms of Foam Flow in Porous Media: Apparent Viscosity in Smooth Capillaries. SPE Journal, **25** (2):176-190.

Green, D.W. and Willhite, G.P. 1998. Enhanced Oil Recovery. Volume 6, SPE Textbook Series, Richardson, Texas: SPE.

Haugen, Åsmund, Martin A. Fernø, Arne Graue, and Henri J. Bertin. 2012. Experimental Study of Foam Flow in Fractured Oil-Wet Limestone for Enhanced Oil Recovery. SPE Reservoir Evaluation & Engineering **15** (2). SPE-129763-PA.

Healy, R. N., Holstein, E. D., & Batycky, J. P. 1994. Status of Miscible Flooding Technology. 14th World Petroleum

Congress, 29 May-1 June, Stavanger, Norway. WPC-26169.
Lee, H. O., & Heller, J. P. 1990. Laboratory Measurements of CO_2-Foam Mobility. SPE Journal. SPE-17363-PA.

Li, Robert F., George Hirasaki, Clarence A. Miller, and Shehadeh K. Masalmeh. 2012. Wettability Alteration and Foam Mobility Control in a Layered, 2d Heterogeneous Sandpack. SPE Journal **17** (04). SPE-141462-PA.

Liu, Y., Grigg, R. B., & Bai, B. 2005. Salinity, pH, and Surfactant Concentration Effects on CO_2-Foam. SPE-93095-MS.

Mannhardt, K., Novosad, J., & Schramm, L. 2000. Comparative evaluation of foam stability to oil. SPE Reservoir Evaluation & Engineering, 3 (01), 23-34.

Marsden, S. S., and Suhail A. Khan. 1966. The Flow of Foam through Short Porous Media and Apparent Viscosity Measurements. SPE Journal **6** (01). SPE-1319-PA.

Nikolov, A., Wasan, D., Huang, D., & Edwards, D. 1986. The Effect of Oil on Foam Stability: Mechanisms and Implications for Oil Displacement by Foam in Porous Media. SPE Annual Technical Conference and Exhibition. New Orleans, Louisiana, USA. SPE-15443-MS.

Porter, M. R. 1994. Handbook of Surfactants, Blackie Academic & Professional, United Kingdom.

Rafati, R., Hamidi, H., Idris, A. K., & Manan, M. A. 2012. Application of sustainable foaming agents to control the mobility of carbon dioxide in enhanced oil recovery. Egyptian Journal of Petroleum, **21** (2): 155-163.

Rosen, M. J., & Kunjappu, J. T. 2004. Foaming and Antifoaming by Aqueous Solutions of Surfactants and Interfacial Phenomena John Wiley & Sons, Inc.: 308-335.

Schramm, L. L., & Wassmuth, F. 1994. Foams: Basic Principles Foams: Fundamentals and Applications in the Petroleum Industry. Volume 242, American Chemical Society: 03-45.

Schramm, L.L. Surfactants: Fundamentals and Applications in the Petroleum Industry. 2000. Cambridge University Press: 03-50.

Taber, J.J., Martin, F.D. and Seright, R.S. 1997. EOR Screening Criteria Revisited - Part 1: Introduction to Screening Criteria and Enhanced Recovery Field Projects. SPERE 12 (3): 189-198. SPE-35385-PA.

Talley, L. D. 1988. Hydrolytic Stability of Alkylethoxy Sulfates. SPE-14912-PA.
Zhao, L., Li, A., Chen, K., Tang, J., & Fu, S. 2011. Development and evaluation of foaming agents for high salinity tolerance. Journal of Petroleum Science and Engineering. **81**: 18-23. DOI:10.1016/j.petrol.2011.11.006.